Stability of direct GPS estimates of ocean tide loading

C. R. Allinson, P. J. Clarke, S. J. Edwards, M. A. King

School of Civil Engineering and Geosciences, University of Newcastle upon Tyne, UK

T. F. Baker

Proudman Oceanographic Laboratory, Bidston, UK

P. R. Cruddace

Ordnance Survey, Southampton, UK

Allinson, C. R., P. J. Clarke, S. J. Edwards, M. A. King, T. F. Baker, and P. R. Cruddace (2004), Stability of direct GPS estimates of ocean tide loading, Geophys. Res. Lett., 31, L15603, doi:10.1029/2004GL020588.

Abstract. We observe ocean tide loading (OTL) at diurnal and semi-diurnal periods by directly estimating fixed-period harmonic motions within individual daily GPS analyses. Stacking of multiple solutions allows us to isolate the principal near-diurnal and near-semi-diurnal OTL components. Using data from UK sites where predicted OTL for the M_2 component varies from 3-46 mm in amplitude, we show that our amplitude estimates are stable for the principal OTL components when data from at least 90 days are stacked. Exceptionally, the K_1 and K_2 components require at least 2000 days of data for adequate amplitude resolution. Stability of the phase estimates is similarly reached sooner for the larger-amplitude components. Our final observations are in agreement with OTL predicted by recent tidal models, but differ significantly at some locations from those predicted by the CSR3 and TPXO.2 tidal models.

1. Introduction

The gravitational forces exerted by the Sun and the Moon give rise to periodic deformations of the solid Earth at a number of well-defined frequencies [e.g. *Melchior, 1966*]. Of these deformations, the solid Earth tide caused by the direct gravitational attraction is by far the larger and can be modeled to within typically 2 mm amplitude [*Baker et al.*, 1991], but the smaller and less well-modeled effect induced by the ocean tides' variation in seafloor pressure, known as ocean tide loading (OTL), is significant in many coastal regions [e.g. *Lambert et al.*, 1998]. One such locality is the British Isles, where the effects of an intricate coastline, and the interaction of tides between the open ocean and more restricted nearby seas, contrive to make OTL large in both magnitude and uncertainty.

OTL may be estimated by convolving an ocean tidal model, giving the spatial variation in mass loading at the epoch, with a Green's function, describing the unit impulse response of the Earth to loading as a function of load magnitude and response location [*Farrell*, 1972]. Typically an elastic Earth model with radial structure, such as PREM [*Dziewonski and Anderson*, 1981] is used, in which case the Green's function depends on load-response separation only. Several computer programs are publicly available to carry out these calculations [*Scherneck*, 1991; *Pagiatakis*, 1992; *Agnew,* 1997]. The error in the OTL estimates arises principally from that of the ocean tide models, although the effects of lateral heterogeneity in Earth structure and of anelastic deformation also contribute. These factors are heightened near the coast, because of local errors in the tidal models caused by changes and errors in bathymetry, and smaller scale hydrodynamic effects that are omitted from the models, and because of local errors in the Green's functions due to the lateral variation in Earth structure across the transition from oceanic to continental lithosphere.

OTL displacements, which are largest in the vertical but also affect lateral position, are in principle detectable by all modern space geodetic techniques. OTL is particularly important for microwave-based methods because of the trade-off that occurs between the estimated station height and tropospheric zenith wet delay (ZWD) parameters [*Dragert et al.,* 2000; *Vey et al.,* 2002]. If the ZWD is regarded as more than just a nuisance parameter, then it is important to have good models of OTL. Moreover, for campaign-style GPS measurements with short occupation times, the positional bias caused by OTL may in itself overwhelm all other error sources, while any mismodelled component of OTL will alias into continuous GPS time series [*Penna and Stewart*, 2003].

We therefore seek direct observations of OTL displacement in the British Isles from long time series of GPS observations. In estimating OTL directly, we must be careful to avoid contamination by tropospheric effects, and to use a long enough dataset to enable the various frequency components of OTL to be separated from each other and from noise. The primary aim of this paper is to show how long this dataset must be.

2. GPS Observations and Processing Strategy

Since 2000, the Ordnance Survey (OSGB) has maintained a growing "Active Network" of up to 30 continuously-operating GPS stations spanning Great Britain. Each site has a dual-frequency receiver mounted on a purpose-built structure or stable building, and data are now archived at the NERC British Isles GPS Facility (http://www.bigf.ac.uk). We selected seven of these sites (Figure 1), each with a long history of continuous high-quality observations, for use in this study. Sites were chosen to include a mixture of inland and coastal locations, with a range of predicted OTL amplitudes.

We processed a ~1000-day span of GPS data from each site using the "Precise Point Positioning" (PPP) mode of the GIPSY/OASIS II software [*Zumberge et al.*, 1997]. PPP utilizes precise satellite orbit and clock data from a previous global network solution (in our case, the JPL "Final" precise orbit determination) to allow coordinates of GPS receivers to be obtained on an individual basis, typically with few-mm precision, from 24-hour datasets. In our solutions, we used a 10° elevation mask, a 5 minute data interval, and modeled tropospheric ZWD as a random-walk parameter with process noise 6 mm/√hr. Carrier phase ambiguities were not resolved. A single set of site coordinates was estimated for each day. Pole and solid Earth tides were modeled [*Melchior*, 1966], but no a priori OTL model was removed. Instead, sub-daily OTL was estimated as a set of harmonic motions (amplitudes of sine and cosine components) in each of the local east, north and up directions, with periods corresponding to the M_2, S_2, N_2, K_2, K_1, O_1, P_1, and Q_1 tides [*Sovers*, 1994].

3. Solution Stacking and Stability

Harmonic motion amplitude estimates and their full variance-covariance matrix (VCM) were extracted from each daily site solution. These were then combined for the full 1000-day span at each site to get our "true" estimates of amplitude and phase for each OTL component. For this combination, we used an iterative Kalman filtering algorithm which updates a daily scale factor for the VCMs at each iteration. Next we chose 20 random subsets of each of $N = 1, 2, \ldots 200$ continuous days' estimates from our dataset, and re-estimated the OTL using only that subset of the data. At this point we calculated the nodal corrections [*Scherneck*, 1999] for each day in the combination, and applied a mean correction to the final N-day result. For each set of N-day estimates we then calculated the mean absolute difference from the "true" estimate, for the amplitude, phase, and complex-valued amplitude of each OTL component. The complex-valued amplitude and phase results for the vertical component of the LEED station are presented in Figure 2. The LEED site was selected as representative of the results from all stations, as can be seen from the M_2 signal convergence for all seven locations in Figure 3. Only the vertical component of the results is discussed here, as the north and east results follow similar trends in stability but are generally less well resolved because they are significantly smaller in magnitude (typically <25% of that of the vertical signal).

The complex-valued amplitude for the ABER station appears to suffer from large fluctuations during this 200-day period when compared with the other sites (Figure 3). However, the estimates appear to start to converge with 175 or more days of data in the solution. The requirement for a larger volume of data is thought to be due to lower signal/noise at this location. Inspection of the complex-valued amplitude reveals that estimates of the M_2, S_2 and N_2 harmonics converge earlier (after ~90-days) than the K_2, K_1 and P_1 estimates. This pattern is illustrated in the phase component of the signals, where generally the larger magnitude, mostly semi-diurnal, phase components also converge at ~90-day span (producing an M_2 RMS phase misfit of ~6°). The smallest magnitude diurnal constituents (P_1 and Q_1) do not converge during the 200-day period.

4. Comparison with Tidal Models

The estimates from the 1000-day span solutions were then compared to OTL predicted by a range of existing models (*Agnew* [1997]; FES95.2, FES99, GOT00.2, TPXO.2, TPXO.6, NAO.99b and CSR3 [*Baker et al.*, 2003]), results of which are presented in phasor-plot format in Figure 4. Agreement between the model estimates and our final 1000-day estimates is good for the larger magnitude constituents, with an M_2 amplitude misfit of ~0.5mm (~5% of the total signal) from the FES99 model at the LEED station (FES99 consistently shows good agreement across the eight stations). In contrast, the TPXO.2 model produces an amplitude M_2 misfit of ~1.9mm (~19% of the total signal), which is consistently the worst model, ranking alongside CSR3. This result is not unexpected since TPXO.2, CSR3 and FES95.2 have significantly less data assimilated than the other, more recent, models.

Figure 4 illustrates much larger disagreement among the smaller magnitude diurnal signals (and also the K_2 constituent) and models, especially in the phase. Even with the full 1000-day span of data in the solution, the phase misfits are typically in excess of 100° for K_2, with consistent over-estimation of the amplitude (misfit values are approximately a factor of four greater than the modeled magnitude of the signal). Phase misfits remain 10-50° for the K_1, and P_1 harmonics, with amplitude misfit values approximately twice the magnitude of the modeled signal (although model predictions are almost within the GPS error ellipses at the 95% confidence level).

Model comparison of the observed K_1 and K_2 signals generally show a perhaps-unexpected large amplitude misfit, and tests (not shown) reveal that more than 2000 days of data are required in the combination for an acceptable resolution of these components (and also for the diurnal P_1 component). The K_1 and K_2 harmonics are very difficult to separate from multipath bias during the processing stage of the estimation strategy, and are therefore much more difficult to determine with the same level of confidence.

5. Conclusions

The purpose of this study was to show that OTL components may be directly estimated from GPS data via a modified GPS processing strategy. This approach has distinct advantages over other methods which use sub-daily solutions [*Dragert et al*., 2000] since the long data arcs are preserved in our approach and ambiguities do not need to be resolved to obtain bias-free horizontal estimates [*King et al*., 2003]. Another aspect was to establish the amount of data required for the adequate resolution of these OTL components, in order to minimize processing time, and maximize efficiency.

We have shown that the Kalman filter estimation method requires a minimum of ~90 days of data to sufficiently resolve the principal semi-diurnal and diurnal OTL components. The resulting accuracy associated with these estimates should be ~10% of the true value, as shown in the test results. This approach can be used for the determination of these OTL parameters at temporary stations, at locations where current 'gaps' exist in permanent GPS networks and OTL modeling is suspected to be deficient. To resolve the K_2, K_1 and P_1 components with a similar level of confidence, a significantly larger data-set is required. This is mainly due to the smaller magnitude of these signals, and the presence of multipath and related errors. These factors combine to necessitate data spans in excess of 2000 days in order to reliably resolve these OTL components, which is at present unrealistic at the majority of locations. Temporary stations can therefore only be used to estimate the M_2, S_2, N_2 and O_1 harmonics, due to time limitations in data collection and the associated inaccuracies with short data-span periods.

Acknowledgments. This work was funded by the UK Natural Environment Research Council, grant NER/A/S/2000/01317. PJC acknowledges sabbatical travel funds from CIRES, University of Colorado. We thank the NERC British Isles GPS facility (BIG F) for provision of data and JPL for the provision of orbit and clock products. Xiaoping Wu kindly provided modified GIPSY routines for estimating the OTL constituents.

References

Agnew, D. C., NLOADF: A program for computing ocean-tide loading, *J. Geophys. Res.*, 102, 5109–5110, 1997.

Baker, T.F., and M.S. Bos, Validating Earth and ocean tide models using tidal gravity measurements, *Geophysical Journal International*, *152* (2), 468-485, 2003.

Baker, T. F., R. J. Edge, and G. Jeffries, Tidal gravity and ocean tide loading in Europe, *Geophys. J. Int.,* 107**,** 1–11, 1991.

Dragert, H., T. S. James, and A. Lambert, Ocean loading corrections for continuous GPS, *Geophys. Res. Lett.,* 27(14), 2045–2048, 2000.

Dziewonski, A. D. and D. L. Anderson, Preliminary Reference Earth Model, *Phys. Earth planet. Inter.,* 25**,** 297–356, 1981.

Farrell, W. E., Deformation of the Earth by surface loads, *Rev. Geophys. Space Phys.,* 10**,** 761–797, 1972.

King, M., R. Coleman, and L. Nguyen, Spurious periodic horizontal signals in sub-daily GPS position estimates, *Journal of Geodesy*, *77* (1-2), 15-21, doi:10.1007/s00190-002-0308-z, 2003.

Lambert, A., S. D. Pagiatakis, A. P. Billyard, and H. Dragert, Improved ocean tide loading corrections for gravity and displacement: Canada and northern United States, *J. Geophys. Res.,* 103**,** 30,231–30,244, 1998.

Melchior, P., *The Earth Tides*, 114 pp., Pergamon Press, New York, New York, 1966.

Pagiatakis, S. D., Program LOADSDP for the calculation of ocean load effects, *Manusc. Geod.*, 17, 315-320, 1992

Penna, N.T., and M.P. Stewart, Aliased tidal signatures in continuous GPS height time series, *Geophys. Res. Lett.*, *30* (23), 2184, doi:10.1029/2003GL018828, 2003.

Scherneck, H. G., A parameterized solid Earth tide model and ocean tide loading effects for global geodetic baseline measurements, *Geophys. J. Int.*, 106, 677-694, 1991.

Scherneck, H.G., Explanatory supplement to the section "Local site displacement due to ocean loading" of the IERS conventions (1996), in Explanatory supplement to the IERS Conventions (1996) chapters 6 and 7, edited by H. Schuh, pp.29, Deutsches Geodätisches Forschungsinstitut, München, 1999.

Sovers, O.J., Vertical ocean loading amplitudes from VLBI measurements, *Geophys. Res, Lett,*, *21* (5), 357-360, 1994.

C. R. Allinson, P. J. Clarke, S. J. Edwards, M. A. King: School of Civil Engineering and Geosciences, University of Newcastle upon Tyne, Newcastle NE1 7RU, UK; e-mail C.R.Allinson@ncl.ac.uk.

T. F. Baker: NERC Proudman Oceanographic Laboratory, Bidston Observatory, Birkenhead CH43 7RA, UK.

P. R. Cruddace: Ordnance Survey, Romsey Road, Southampton SO16 4GU, UK.

(Received November XX, 2003; revised November XX, 2003;
accepted December XX, 2003.)

AGU Copyright:

Paper number 2003GLxxxxxx.

0094-8276/01/2003GLxxxxxx$05.00

****Provide running head (45 character max for short title):**

ALLINSON ET AL.: STABILITY OF GPS OCEAN TIDE LOADING ESTIMATES

Figure 1. The location of seven continuously operating GPS receivers used to directly measure OTL in the British Isles. Contours show the OTL M_2 amplitude (mm) throughout the British Isles, predicted by the FES99 model.

Figure 2. Convergence graphs for the LEED station, showing N-day RMS misfit relative to the "true" 1000-day estimates. Graphs read (from bottom left, clockwise): semi-diurnal complex-valued amplitude misfit, diurnal complex-valued amplitude misfit, diurnal phase misfit and semi-diurnal phase misfit. The lower, semi-diurnal, graph symbols are: solid line = M_2, broken line = S_2, solid circles = N_2 and open triangles = K_2. The upper, diurnal, graph symbols are: solid line = K_1, broken line = O_1, solid circles = P_1 and open triangles = Q_1.

Figure 3. Convergence graph showing the M_2 complex-valued amplitude misfit, for the vertical OTL component. The results for the LEED station are shown in the solid thick line, while the other station results are shown as broken lines.

Figure 4. Phasor plots for the LEED station showing our 1000-day GPS estimates (thin line with solid circle) and associated error ellipses (95% confidence). A common scale is used on both axis (indicated on the x-axis of the plots). Predicted results for each component are from the FES99 (triangle), FES95.2 (square), CSR3 (circle), TPXO.2 (cross), TPXO.6 (hexagon) models (predictions from GOT.002 and NAO99 are omitted, as they follow a very similar trend to that of TPXO.6).

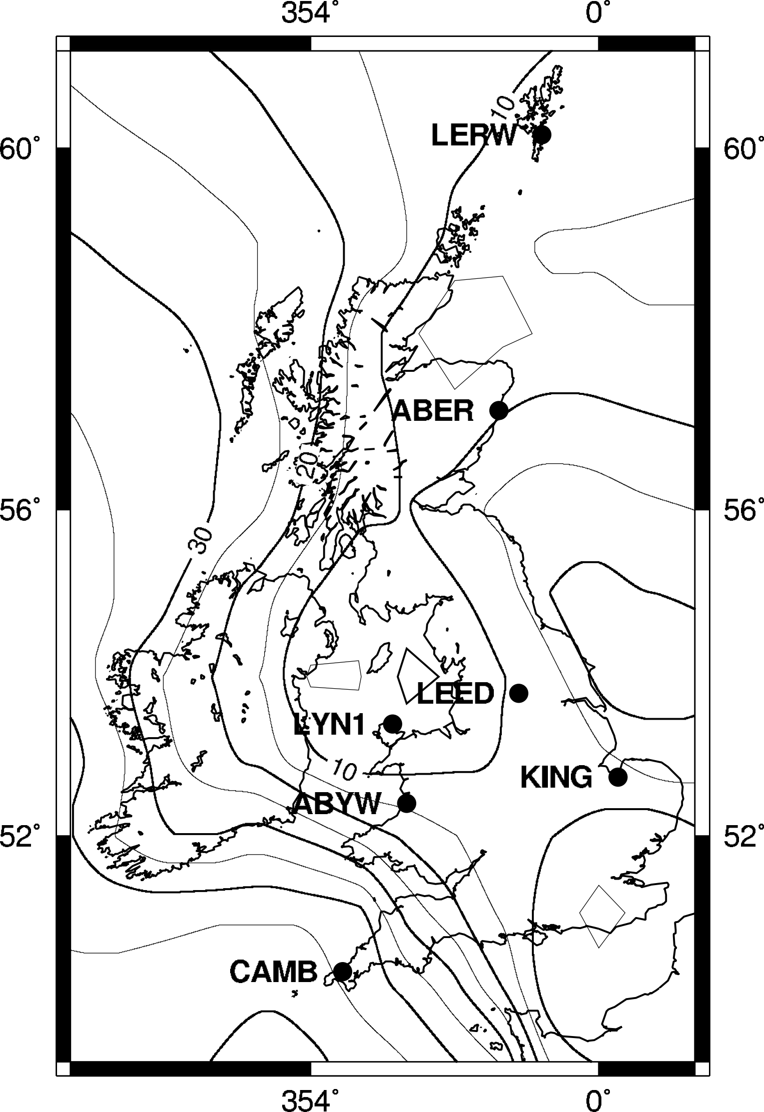

354°
0°
60°
60°
56°
56°
52°
52°
354°
0°
LERW
ABER
LEED
LYN1
ABYW
KING
CAMB
10
20
30
10

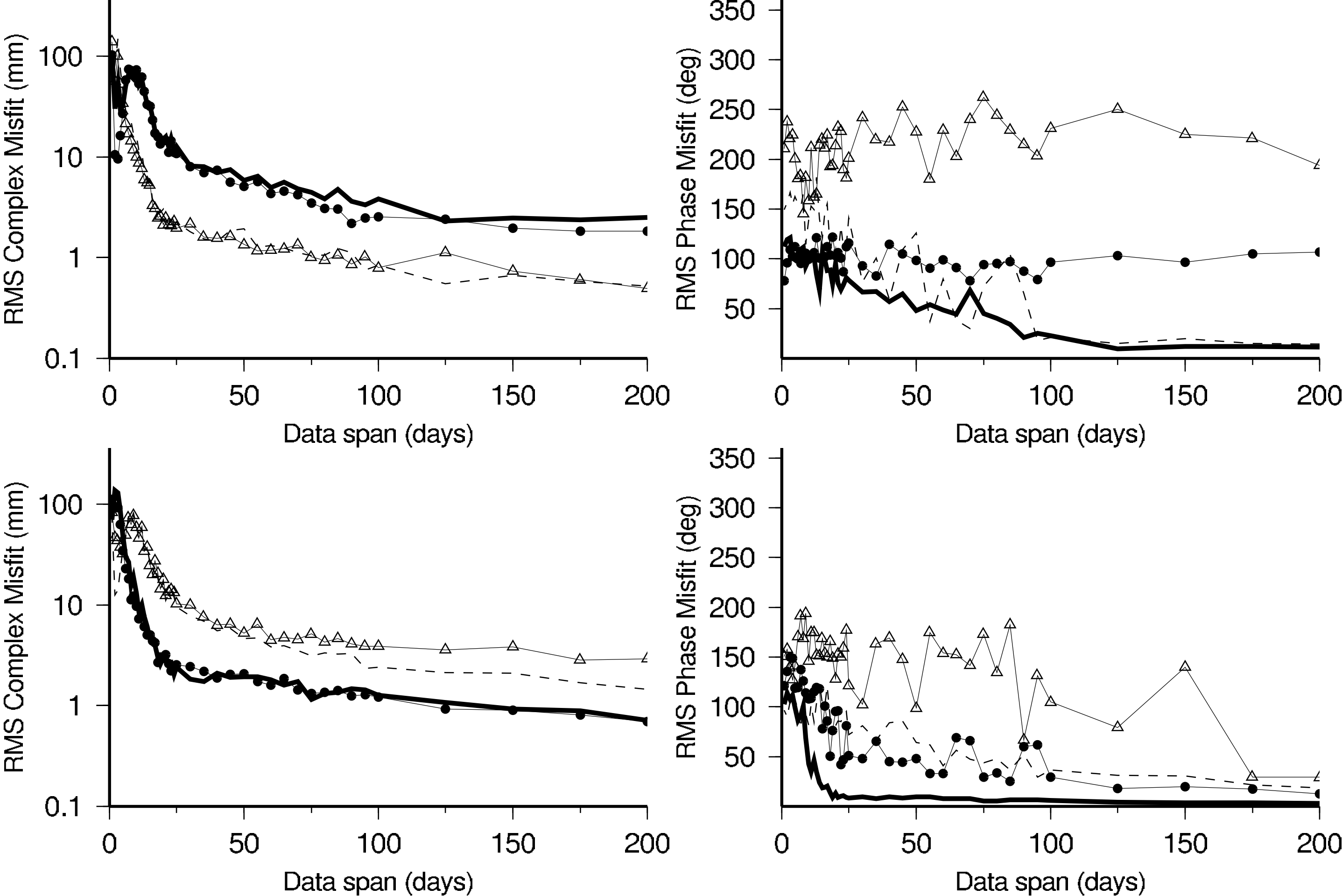

RMS Complex Misfit (mm)
RMS Phase Misfit (deg)
Data span (days)

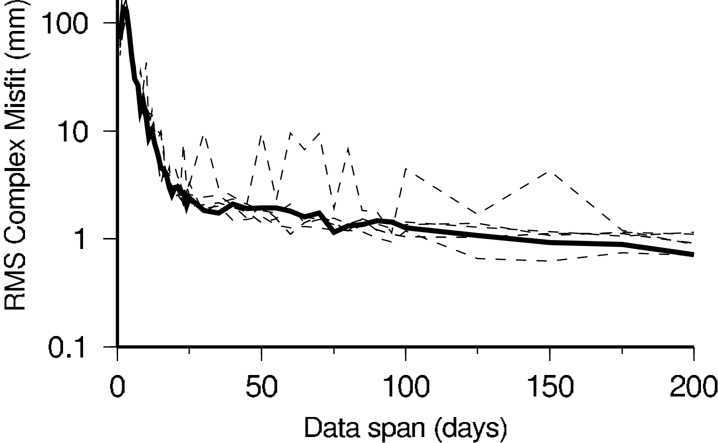

100
10
1
0.1
RMS Complex Misfit (mm)
0
50
100
150
200
Data span (days)

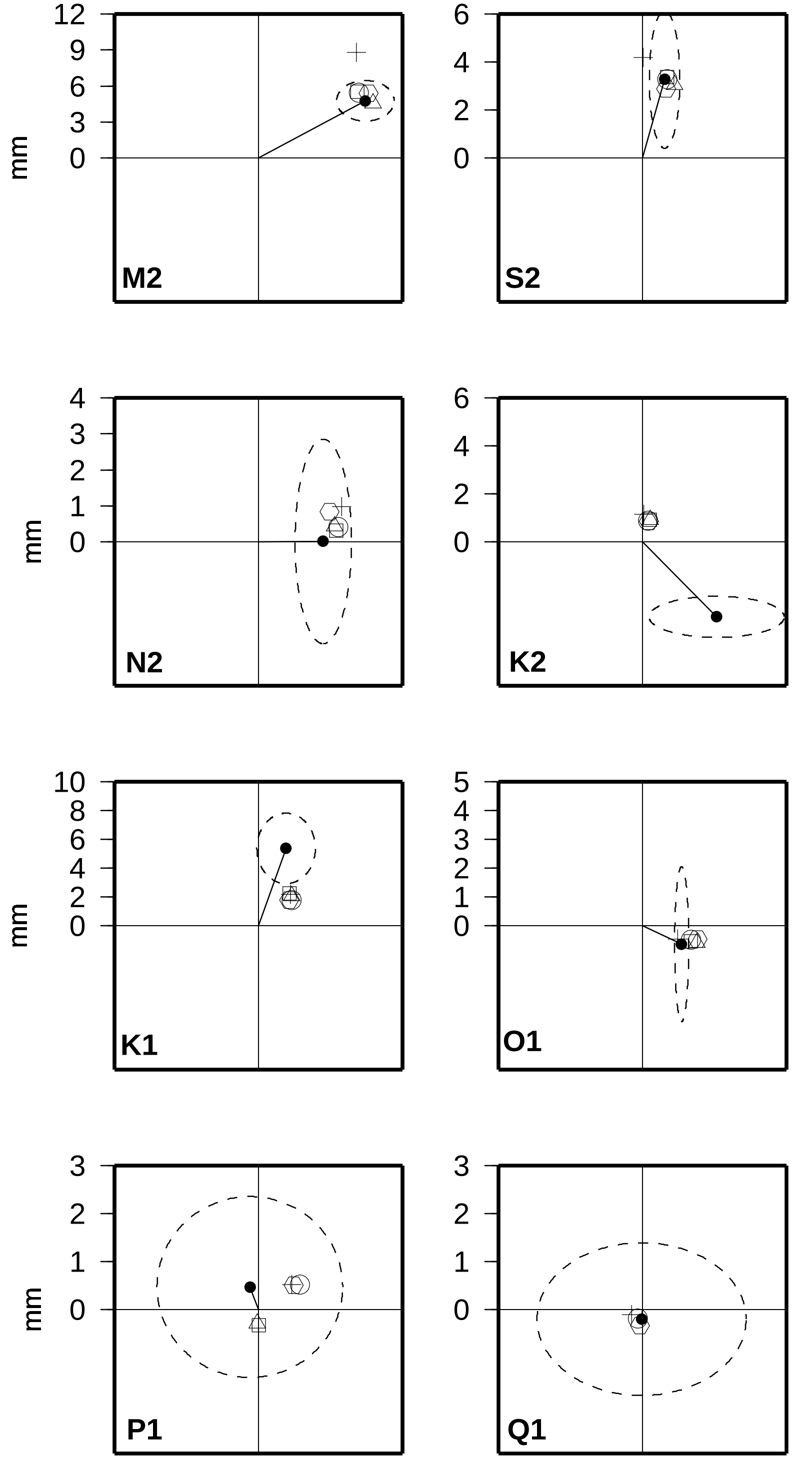

12
9
6
3
0
mm
M2
6
4
2
0
S2
4
3
2
1
0
mm
N2
6
4
2
0
K2
10
8
6
4
2
0
mm
K1
5
4
3
2
1
0
O1
3
2
1
0
mm
P1
3
2
1
0
Q1